Molecular Crystals and Liquid Crystals
Publication details, including instructions for authors and subscription information:
http://www.tandfonline.com/loi/gmcl20

Defect Mode in Axially Deformed Cholesteric Elastomers

L. O. Palomares [a] & J. A. Reyes [a b]

[a] Física Química, Instituto de Física, Universidad Nacional Autónoma de México, México D. F., Mexico

[b] Universidad Autónoma Metropolitana Ixtapalapa, México D. F., Mexico

Version of record first published: 14 Jun 2011

To cite this article: L. O. Palomares & J. A. Reyes (2011): Defect Mode in Axially Deformed Cholesteric Elastomers, Molecular Crystals and Liquid Crystals, 544:1, 203/[1191]-212/[1200]

To link to this article: http://dx.doi.org/10.1080/15421406.2011.569475

Mol. Cryst. Liq. Cryst., Vol. 544: pp. 203/[1191]–212/[1200], 2011

ISSN: 1542-1406 print/1563-5287 online
DOI: 10.1080/15421406.2011.569475

Taylor & Francis
Taylor & Francis Group

Defect Mode in Axially Deformed Cholesteric Elastomers

L. O. PALOMARES[1] AND J. A. REYES[1,2]

[1]Física Química, Instituto de Física, Universidad Nacional Autónoma de México, México D. F., Mexico
[2]Universidad Autónoma Metropolitana Ixtapalapa, México D. F., Mexico

We consider an axially elongated (or stretched) cholesteric elastomer, prolate or oblate, containing a spaceless twist defect. We show that the wavelength of its localized mode can be tuned by either axially compressing (or enlarging) the elastomer or by changing its pitch. We calculate the dwell time given by the inverse relative line width and exhibit that it is enhanced when the values of the deformation and pitch are near a locus in the parameter's sample that we call the pseudo-isotropic curve. We also show the density of states diverges in the pseudo-isotropic curve.

Keywords Cholesteric elastomers; defect mode; dwell time; elastically tuned; twist defect

1. Introduction

Photonic band gap materials with periodicity in one, two or three dimensions offer control of spontaneous emission and photon localization. Yablonovitch has predicted that the lasing threshold can be reduced by introducing a defect into an otherwise periodic band gap structure. Since spontaneous emission is suppressed in the band gap, excitation will not be drained by modes others than the lasing mode [1]. Moreover, the long dwell time of such localized defect modes reduces the gain required to reach the lasing threshold. The photonic dwell time at resonance with a defect increases exponentially with the structure thickness. This suppresses the lasing threshold in an active structure without the use of external feedback.

Periodic chiral media appear in nature as cholesteric liquid crystals [2], synthesized as chiral elastomers [3], or fabricated by glancing-angle deposition on a rotating substrate [4]. Some years ago, low threshold lasing was observed at the band edge of dye doped cholesteric liquid crystals where the dwell time for emitted photons is increased [5].

Kopp and Genack have shown that a defect mode in a cholesteric presents an anomalous crossover in propagation. The twist defect gives rise to a peak in

Address correspondence to J. A. Reyes, Física Química, Instituto de Física, Universidad Nacional Autónoma de México, Apartado Postal 20 364, C.P. 01000, México D.F., Mexico. Tel.: +52 55 56 225178; Fax: +52 55-5625622-5008; E-mail: adrian@fisica.unam.mx

transmission whose inverse relative line width scale exponentially for circularly polarized light with the same handedness as the structure [6]. The photonic dwell time also scales exponentially [7] but, after a crossover thickness of the sample, its value asymptotically approaches to a bound. On the other hand, it has been shown [10] that the band gap and transmittance of a Cholesteric Elastomer CE can be controlled by elongating the material along its helix axis. Furthermore, the deformation was found to close the band gap. This effect is a consequence of the presence of optical axis in the locally anisotropic material forming the CE, which in turns originates the existence of pseudo-isotropic points [9].

2. Model and Governing Equations

In this work we show that the peak line width associated with the defect mode in an elongated cholesteric elastomer including a spaceless twist defect (see Fig. 1), diverges when the elastomer is mechanically tuned near a pseudo-isotropic curve. This critical tuning leads to a tremendous change in the scaling of the photonic dwell time of the defect mode which does not present a crossover thickness and then always increases as a function of the thickness sample [10].

2.1. *Elastic Energy*

A monodomain cholesteric elastomer subject to the action of a longitudinal elongation is described by the microscopic statistical-mechanical theory of rubber elasticity [3] of nematic rubber elasticity energy density which in turns leads to the so called as the trace formula given by

$$F = \frac{1}{2}\mu \,\mathrm{Tr}[l_o \boldsymbol{\eta}^T l^{-1} \boldsymbol{\eta}] \tag{1}$$

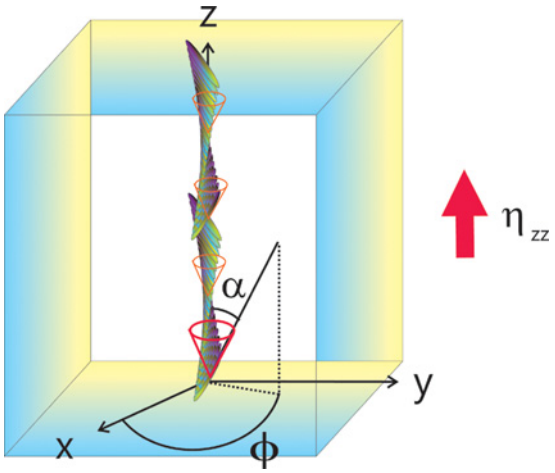

Figure 1. Schematic plot of an axially elongated chiral elastomer containing a discontinuity defect on its helix and characterized by a tilt angle α. (Figure appears in color online.)

where $\boldsymbol{\mu} = n_s \boldsymbol{\kappa}_B T$ is the rubber shear modulus, n_s is the number of chains strands per unit of volume, $\boldsymbol{\kappa}_B$ is the Boltzmann constant, T is the temperature, Tr stands for the trace of the tensor and the local step-length tensors for a locally uniaxial medium are

$$l_0 = \delta + (r-1)\mathbf{n}_0\mathbf{n}_0 \tag{2}$$

$$l^{-1} = \delta + (1/r-1)\mathbf{n}\mathbf{n} \tag{3}$$

where $r = l_{\parallel}/l_{\perp}$ is the fractional shape anisotropy.

In deriving Eq. (1) the entanglements, finite extensibility and semi-softness have been ignored. Here, the director corresponding to the initial configuration is denoted by

$$\mathbf{n}_0 = (\cos\phi - 0, \sin\phi_0, 0),$$

where the angle $\phi^0 = q_0 z$ has a helix wave number $q_0 = 2\pi/p$ and a spatial periodicity or pitch p. This is determined by the concentration and the helical twisting power [11] of the chiral constituents. After the deformation the director is aligned along the surface of a cone, that is

$$\mathbf{n} = (\sin\alpha\cos qz, \sin\alpha\sin qz, \cos\alpha)$$

where α is the azimuthal angle.

When the elastomer is subjected to a mechanical strain a selected chain's end-to-end vector, **R**, will deform proportionally to the body's deformation. The proportionality factor is given by the deformation tensor; $\boldsymbol{\eta}$, which in the case of an expansion parallel to the helix axis, z, $\boldsymbol{\eta}$, has the form [3]:

$$\boldsymbol{\eta} = \begin{pmatrix} \frac{1}{\sqrt{\eta}} & & \eta_{xz} \\ & \frac{1}{\sqrt{\eta}} & \eta_{yz} \\ & & \eta \end{pmatrix} \tag{4}$$

where we have used $\eta_{zz} = \eta$. This expression preserves the volume since by construction $\mathrm{Det}(\boldsymbol{\eta}) = 1$. There is no compatibility inconsistency due to the z-dependence of the elongations η_{xz} and η_{yz}. In contrast, the z-dependence of their conjugate strains η_{zx} and η_{zy} leads to compatibility mismatch as for instance

$$\frac{\partial \eta_{zx}}{\partial z} = \frac{\partial \eta_{zz}}{\partial x}$$

so we suppress them. Finally, η_{xy} and η_{yx} could exist but numerical test [12] suggests that it is not possible. The two shear strains η_{xz} and η_{yz} should be proportional each other so that they are part of a shear in the plane of $\mathbf{n}_0$ and **n** and help to accommodate the rotation of the chain distributions and in turn keep the elastic energy low, as the initial direction and the plane of rotation of **n** changes. All physical dimensions in the deformed sample are assumed to scale by the affine strain as $z \rightarrow z/\eta$ resulting in the corresponding expansion of the cholesteric pitch $q = q_o/\eta$.

Using the above equations, the free energy for an elastomer under mechanical stress can be obtained. Thus, by minimizing the free Helmholtz energy first with respect to the strains η_{xz} and η_{yz} and then with respect to α to obtain:

$$\alpha = \frac{\pi}{2} - \arcsin\sqrt{\frac{\eta^{3/2} - 1}{r - 1}} \tag{5}$$

From this equation follows that the nematic's vector will be totally aligned with the z-axis for the critical longitudinal stress which is equal to,

$$\eta_m = r^{2/3}. \tag{6}$$

Figure 2 shows α versus η for various values of r. We consider the oblate and prolate cases, with the corresponding ranges: a) $0 < r \leq \eta^{3/2} < 1$ (for a given η), with $0 < \eta_m \leq \eta < 1$ (for a given r), and correspondingly b) $1 \leq \eta^{3/2} \leq r$ with $1 \leq \eta \leq \eta_m$. This plots clearly exhibits that for an oblate cholesteric elastomer, α goes from 0 to $\pi/2$ for the interval $0 < \eta_m \leq \eta < 1$ for a fixed value of r, and α monotonically decreases towards 0 in the interval $0 < r \leq \eta^{3/2} < 1$, for a fixed value of η. On the other hand, for a prolate CE, α monotonically decreases from $\pi/2$ to 0 while η increases its value from 1 to η_m, for some value of $r > 1$, and α increase its value from 0, when r increase for $1 \leq \eta^{3/2} \leq r$, with η fixed. Once the elastomer has reached the critical strain η_m, α remains in the same value 0.

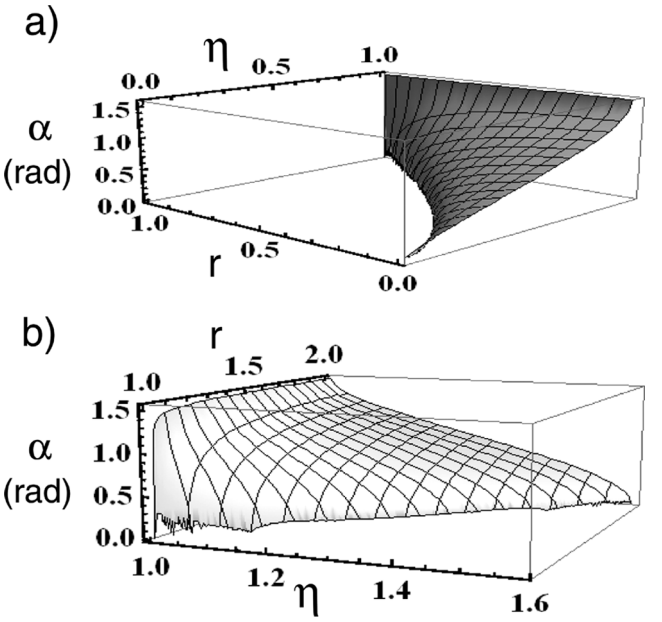

Figure 2. Tilt angle α describing a stretched chiral elastomer subjected to an axial elongation η. We consider both cases a) an oblate and b) a prolate elastomer. Other parameters are $L = 10.7\,\mu m$, $(p/2) = 214\,nm$, $\varepsilon_\perp = 1.91$, $\varepsilon_\parallel = 2.22$, $\mu = 1$, which correspond for $r = 1.16$ to a real sample made by a siloxane backbone chain reacting with 90 mol % and 10% of the flexible dysfunctional cross-linking groups (di-11UB).

2.2. *Optical Modes*

Equation (5) provides a expression for determine the director vector, **n**, which allows us to find the dielectric tensor of the elastomer:

$$\boldsymbol{\varepsilon} = \varepsilon_{\perp}\delta_{ij} + \varepsilon_a \mathbf{nn},$$

where $\varepsilon_a = \varepsilon_{\parallel} - \varepsilon_{\perp}$, is the dielectric anisotropy, $\varepsilon_{\parallel}$ and $\varepsilon_{\perp}$ are the dielectric constants parallel and perpendicular to the director **n**.

Maxwell equations for the selected structurally chiral material and normally incident monochromatic plane wave are only z-dependent. Hence, they can be solved in terms of

$$\psi(z) = \begin{pmatrix} e_x(z) \\ e_y(z) \\ h_x(z) \\ h_y(z) \end{pmatrix},$$

where $e_x(z)$, $e_y(z)$, $h_x(z)$ and $h_y(z)$ are the transverse components of the electromagnetic fields. Using the Oseen transformation and following a very well known procedure [13], it can be established that $\psi(z)$ satisfies:

$$\frac{d\psi(z)}{dz} = iA\psi(z)$$

where A is given by

$$A = \begin{pmatrix} 0 & iq & 0 & -\omega\mu_0 \\ -iq & 0 & \omega\mu_o & 0 \\ 0 & \omega\varepsilon_o\varepsilon_{\perp} & 0 & iq \\ -\omega\varepsilon_o\varepsilon_d(\eta, r) & 0 & -iq & 0 \end{pmatrix} \tag{7}$$

Here μ_o and ε_o are the magnetic permeability and dielectric permittivity of vacuum whereas

$$\varepsilon_d(\eta, r) = \frac{\varepsilon_{||}\varepsilon_{\perp}(r-1)}{\varepsilon_{||}(\eta^{3/2}-1) + \varepsilon_{\perp}(r-\eta^{3/2})} \tag{8}$$

Notice that A does not depends on z. Thus, the eigenvalues of A allow us to determine the wave numbers: The eigenvalues of A are given by

$$k_{\pm}^2 \equiv q^2 + \frac{1}{2}(\varepsilon_d(\eta, r) + \varepsilon_{\perp})\left(\frac{\omega}{c}\right)^2 \pm \frac{1}{2}\left(\frac{\omega}{c}\right) \times \sqrt{8q^2(\varepsilon_d(\eta, r) + \varepsilon_{\perp}) + \left(\frac{\omega}{c}\right)^2(\varepsilon_d(\eta, r) - \varepsilon_{\perp})^2} \tag{9}$$

Only the modes k_- and $-k_-$ show a bandgap for ω within the interval defined by the positive roots of the equation $k_-^2 = 0$. The band edges in terms of their corresponding wavelengths are given by $\lambda_1 \equiv 2\pi\eta\sqrt{(\varepsilon_{\perp}/q_o}$ and $\lambda_2 \equiv 2\pi\eta\sqrt{\varepsilon_d(\eta)}/q_o$. In this band gap

the modes $\pm k_-$ are pure imaginary and their corresponding eigenvectors are linearly polarized. Thus, the central wavelength of the bandgap is

$$\lambda = \frac{\lambda_1 + \lambda_2}{2} = \pi\eta \frac{\sqrt{\varepsilon_\perp}}{q_o} \left(1 + \sqrt{\frac{r-1}{(\eta^{3/2}-1) + \frac{\varepsilon_\perp}{\varepsilon_{||}}(r-\eta^{3/2})}} \right). \tag{10}$$

It can be shown straightforwardly [8] and experimentally [14] that for a prolate anisotropic elastomer, the reflected wavelength λ increases by stretching the sample along the helix axis.

Let us consider that the lossless helical structure is bounded between the planes $z=-l$ and $z=l$ with a discontinuity plane at $z=0$, such that the optical axes at the two sides of the plane make a twist angle ϕ. The electromagnetic field can be written as the linear superposition of the four eigenmodes $\tilde{\alpha}_\pm^\pm$ whose eigenvalues are defined by Eq. (9)

$$f_\alpha(z) = a_-^+ \tilde{\alpha}_-^+ e^{-ik_- z} + a_-^- \tilde{\alpha}_-^- e^{-ik_- z} + a_+^+ \tilde{\alpha}_+^+ e^{-ik_+ z} + a_+^- \tilde{\alpha}_+^- e^{ik_+ z}, \qquad z < 0$$
$$f_\beta(z) = b_-^+ \tilde{\beta}_-^+ e^{-ik_- z} + b_-^- \tilde{\beta}_-^+ e^{-ik_- z} + b_+^+ \tilde{\beta}_+^+ e^{-ik_+ z} + b_+^- \tilde{\beta}_+^+ e^{ik_+ z}, \qquad z > 0$$

where the eigenmodes $\tilde{\beta}_\pm^\pm$ can be obtained from $\tilde{\alpha}_\pm^\pm$ by applying a rotation by an angle ϕ to the vectors **e** and **h**. If we consider the extreme case of an unbounded helix, namely in the limit $l \to \infty$, the coefficients of the exponentially diverging eigenmodes must be zero ($a_-^+ = b_-^- = 0$). The coefficients a_-^- and b_-^+ define a localized mode, which depends on z as $\exp(-|z|l_d^{-1})$, where the inverse of the line width is defined by $l_d^{-1} = |k_-|$, whereas the coefficients a_+^+ and b_+^+ define a nonlocalized component. The six nonzero coefficients must satisfy the boundary continuity conditions prescribed by the continuity of the tangential components of the electromagnetic fields that is $f_\alpha(0) = f_\beta(0)$. For any ω within the gap they admit solutions with $a_-^- = b_-^+ = 1$ and $|a_+^+| = |a_+^-| = |b_+^+| = |b_+^-| = m(\omega)$. The ratio $\rho(\omega) = 1/2m^2$ between the square amplitudes of the localized and travelling components has an enhanced maximum for a given frequency ω_d. This solution defines therefore a quasi-localized defect mode with defect frequency ω_d [7]. If the chiral discontinuity angle is $\pi/2$, the peak generated by this defect is located at the central wavelength of the Bragg regime [15]: $\lambda = (\lambda_1 + \lambda_2)/2$ whose band width is: $\Delta\lambda \equiv \lambda_1 - \lambda_2$.

2.3. *Photonic Dwell Time*

The dwell time τ of this defect mode is given by the ratio between the electromagnetic energy stored by the sample and the total power of the outgoing waves. By neglecting the contribution of the propagating waves to the stored energy [7] $\tau(l)$ is given by

$$\tau(l) = \frac{l_d}{4c} \sqrt{\frac{\varepsilon_1^0 + \varepsilon_2^0 + \varepsilon_3^0}{3}} \frac{(1 - \exp(-2l/l_d))}{\sin^2(\gamma_{em}/2) + \exp(-2l/l_d)} \tag{11}$$

whose asymptotic value for a very large sample is $\tau(\infty) = l_d / \left(4c \sin^2(\gamma_{em}/2)\right) \sqrt{\left((\varepsilon_1^0 + \varepsilon_2^0 + \varepsilon_3^0)/3,\right)}$ where $\varepsilon_1^0 = \varepsilon_2^0 = \varepsilon_\perp$ and $\varepsilon_3^0 = \varepsilon_{||}$.

If, however, the CE is tuned on the pseudo-isotropic curve, τ(l) reduces to $\tau(l) = (l/2c)\sqrt{\left((\varepsilon_1^0 + \varepsilon_2^0 + \varepsilon_3^0)/3,\right)}$ which now depends proportionally on the sample thickness and hence never gets bounded as it occurs for a point outside of the mentioned curve. Hence, the photonic dwell time can be prolonged without limit by enlarging the sample thickness l.

3. Results and Discussion

In Figure 3 we depict λ versus η and q_0. This plot show that λ diminishes monotonically from a wavelength in the near infrared ~(1450 nm) to the blue wavelength ~(470 nm), when q_0 increases in the interval for p (1000 nm, 250 nm); for both cases oblate and prolate. Complementary, λ gets larger when the elongation η grows also for both types of elastomers. This suggests a mechanism for tuning mechanically the defect mode of the elastomer.

In ref. [10] we calculated $l_d^{-1}(\omega_d)$, $\Delta\omega$ and $\gamma_{em}(\omega_d)$ versus q_0 and η and showed that there is a locus where all these quantities vanish simultaneously. This signifies that in the mentioned locus that we call pseudo isotropic curve [9] we have the following situation:

i. the transport of waves within the elastomer having the defect frequency is completely efficient since the attenuation for the defect mode is null since this is determined by $l_d^{-1}(\omega_d)$,
ii. the circular Bragg regime closes since the band width vanishes,
iii. For this frequency there are no energy transport in the sample since the electric and magnetic fields are parallel each other so that the Poynting vector is null.

In Figure 4 we draw the inverse relative line width $\omega_d\tau$ as function of η and q_0 for both kinds of elastomers. We notice that $\omega_d\tau$ grows in two orders of magnitude,

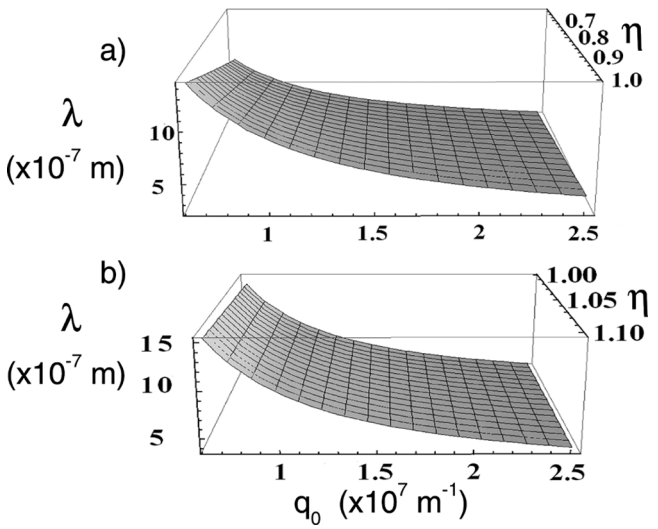

Figure 3. Defect wavelength λ versus q_0 and η for: a) an oblate (r = 0.5) and b) a prolate elongated elastomer (r = 1.16). The same parameters as Figure 2.

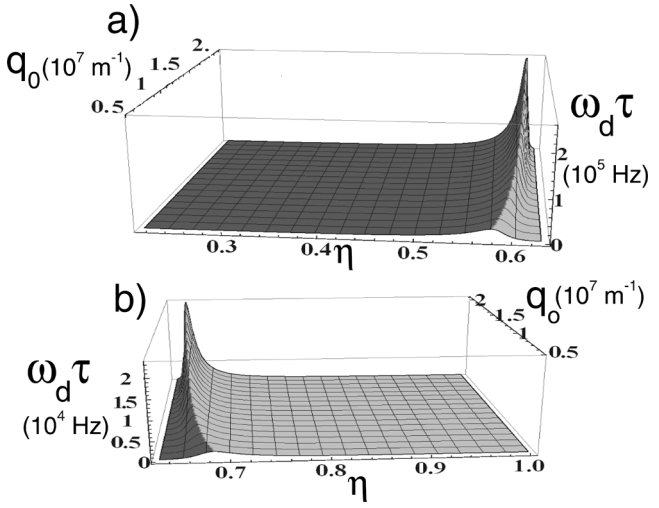

Figure 4. Inverse relative line width $\tau\omega_d$ as a function of q_0 and η for: a) an oblate (r = 0.5) and b) a prolate elongated elastomer (r = 1.16). The same parameters as Figure 2.

more than in the rest of the space $\eta - q_0$, when the parameters η and q_0 are near the pseudo isotropic curve.

Finally, the density of photonic states D at the defect frequency [16] is inversely related with the group velocity.

$$V_g(\omega_d) = l/D(\omega_d) \equiv \frac{\partial \omega_-}{\partial k(\omega_d)} \tag{12}$$

can be analytically obtained from Eq. (9).

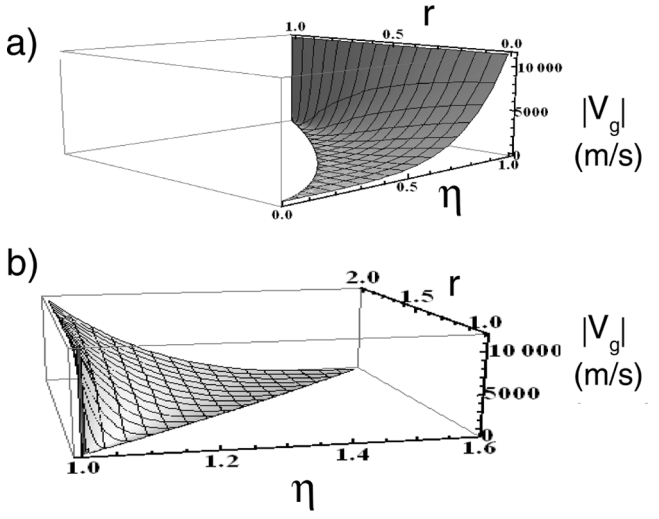

Figure 5. Group velocity against η and r for: a) an oblate and b) a prolate elongated elastomer. The same parameters as Figure 2.

$$V_g = \frac{(\varepsilon_d(\eta,r)+\varepsilon_\perp)\left(-16\pi^2(\varepsilon_d(\eta,r)+\varepsilon_\perp)+p^2\eta^2\left(\frac{\omega}{c}\right)\right)}{\sqrt{2}p\eta\sqrt{(\varepsilon_d(\eta,r)+\varepsilon_\perp)\left(p^2\eta^2\left(\frac{\omega}{c}\right)(\varepsilon_\perp-\varepsilon_d(\eta,r))+32\pi^2\right)}} \times \frac{\left(\frac{\omega}{c}\right)(\varepsilon_d(\eta,r)-\varepsilon_\perp)+\sqrt{(\varepsilon_d(\eta,r)+\varepsilon_\perp)\left(\left(\frac{\omega}{c}\right)^2(\varepsilon_\perp-\varepsilon_d(\eta,r))+\frac{32\pi^2}{p^2\eta^2}\right)}}{\sqrt{\frac{8\pi^2}{p^2\eta^2}+\left(\frac{\omega}{c}\right)(\varepsilon_d(\eta,r)+\varepsilon_\perp)-\left(\frac{\omega}{c}\right)\sqrt{(\varepsilon_d(\eta,r)+\varepsilon_\perp)\left(\left(\frac{\omega}{c}\right)^2(\varepsilon_\perp-\varepsilon_d(\eta,r))+\frac{32\pi^2}{p^2\eta^2}\right)}}} \quad (13)$$

In Figure 5 we present $V_g(\omega_d)$ versus η and r also for both kinds of elastomers. We confirm that this quantity gets null for values of η and r which are in the pseudo isotropic curve, thus the density of photonic states diverges at the defect frequency.

4. Conclusions and Perspectives

In summary, we have considered a cholesteric elastomer having a $\pi/2$ plane-discontinuity on its helix, submitted to a dc field. We have shown that the defect wavelength could be tuned by both changing the pitch or by axially deforming the Cholesteric Elastomer. Moreover, aside the pseudo-isotropic curve in the η-q_0 space, the inverse relative line width, that is proportional to the photonic dwell time, is higher than in the rest of the space. This main result is supported by the following facts, for values of the parameters of the cholesteric elastomer on the pseudo-isotropic curve: the propagation of waves in the sample with the defect frequency is extremely efficient since the attenuation for the defect mode is quite small, due to a vanishing inverse line width. Besides, the angle between the electric and magnetic fields is null, hence the energy loses in the sample are negligible due to an almost vanishing Poynting vector. Finally, the density of photonic states diverges there. We expected that other optically biaxial physical systems as smectics C^* present pseudo-isotropic curves where the optical properties could have a unusual behavior.

References

[1] Yablonovitz, E. (1987). *Phys. Rev Lett.*, *58*, 2059.
[2] de Gennes, P. G., & Prost, J. (1993). *The Physics of Liquid Crystals*, Chapter. 6, Clarendon Press, Oxford, UK.
[3] Warner, M., & Terentjev, E. M. (2003). *Liquid Crystal Elastomers*, Chapter 9, Oxford University Press: Oxford, UK.
[4] Lakhtakia, A., Messier, R., BrettK, M. J., & Robbie, k. (1996). *Innovat. Mater. Res.*, *1*, 165.
[5] Kopp, V. I., Fan, B., Vithana, H. K. M., & Genack, A. Z. (1998). *Opt. Lett.*, *23*, 1707.
[6] Kopp, V. I., & Genack, A. Z. (2002). *Phys. Rev. Lett.*, *89*, 33901.
[7] Becchi, M., Ponti, S., & Reyes, J. A., & Oldano, C. (2004). *Phys. Rev. B*, *70*, 33103.
[8] Reyes, J. A., & Lakhtakia, A. (2006). *Opt. Commun.*, *266*, 565.
[9] Abdulhalim, I. (1999). *Europhys. Lett.*, *48*, 177.
[10] Adriana Mota, E., Laura Palomares, O., & Adrian Reyes, Juan (2010). *Appl. Phys. Lett.*, *96*, 081906.

[11] Chandrasekhar, S. (1997). *Liquid Crystals*, Cambridge University Press: Cambridge.
[12] Mao, Y., Terentjev, E. M., & Warner, M. (2001). *Phys. Rev. E*, *64*, 041803.
[13] Reyes, J. A., & Lakhtakia, A. (2006). *Opt. Commun.*, *259*, 164.
[14] Finkelmann, H., Kim, S. T., Muñoz, A., Palffy Muhoray, P., & Taheri, B. (2001). *Adv. Mat.*, *13*, 1069.
[15] Dixit, M., & Lakhtakia, A. (2008). *Opt. Commun.*, *281*, 4812.
[16] Ashcroft, N. W., & Mermin, N. D. (1976). *Solid State Physics*, Chapter 8, Saunder: Philadelphia.